

***N*-soliton Interactions: Effects of Linear and Nonlinear Gain and Loss**

R. Carretero-González^{1,b)}, V. S. Gerdjikov^{2,3,a)} and M. D. Todorov^{4,c)}

¹*Nonlinear Dynamical Systems Group, Computational Sciences Research Center, and Department of Mathematics and Statistics, San Diego State University, San Diego, CA 92182-7720, USA*

²*Institute of Mathematics and Informatics, Bulgarian Academy of Sciences, 8 Acad. G. Bonchev str., 1113 Sofia, Bulgaria*

³*Institute for Advanced Physical Studies, New Bulgarian University, 21 Montevideo str., 1618 Sofia, Bulgaria*

⁴*Department of Applied Mathematics and Computer Science, Technical University of Sofia, 8 Kliment Ohridski, Blvd., 1000 Sofia, Bulgaria*

^{a)}Corresponding author: vgerdjikov@math.bas.bg

^{b)}URL: <http://nlds.sdsu.edu>; <http://carretero.sdsu.edu/>

^{c)}mtod@tu-sofia.bg

Abstract. We analyze the dynamical behavior of the *N*-soliton train in the adiabatic approximation of the nonlinear Schrödinger equation perturbed simultaneously by linear and nonlinear gain/loss terms. We derive the corresponding perturbed complex Toda chain in the case of a combination of linear, cubic, and/or quintic terms. We show that the soliton interactions dynamics for this reduced PCTC model compares favorably to full numerical results of the original perturbed nonlinear Schrödinger equation.

INTRODUCTION

The nonlinear Schrödinger (NLS) equation [1] is a universal model describing the dynamics of envelope waves in dispersive media [2, 3, 4, 5]. The universality of the NLS derives from the fact that it is the simplest model incorporating nonlinearity that is able to propagate envelope waves and, therefore, the NLS can be considered as the normal form for nonlinear envelope wave propagation. Endowed by this normal form universality, the NLS finds its niche in a wide range of applications including optics [6, 7, 8, 9], Bose-Einstein condensation [10, 11, 12, 13], fluid dynamics and plasma physics [14], and many more. While the Hamiltonian (conservative) version of the NLS has been widely studied and applied in a wide range of scientific disciplines, it has been less studied in the more realistic scenario when loss and/or gain is present in the system under consideration. For instance, the NLS equation is tightly related to other dissipative models, such as the complex Ginzburg-Landau equation [15, 16], which have been extensively used in the context of pattern formation [17, 18] and its applications.

One of the most appealing aspects of the NLS equation is that it supports stable localized solutions in the form of solitons in one space dimension (1D) [2, 14, 19, 20, 21, 22]. These building block solutions come in two different flavors depending on the sign of the nonlinearity. For repulsive (or defocusing) cubic nonlinearity the NLS in 1D admits dark soliton solutions [13], while for attractive (or focusing) cubic nonlinearity the basic nonlinear solution is the bright soliton. In the present paper we aim to study the dynamics of interacting bright solitons in the presence of non-conservative terms. Specifically, we consider the focussing NLS equation:

$$iu_t + \frac{1}{2}u_{xx} + |u|^2u(x, t) = iR[u]. \quad (1)$$

with, non-conservative, perturbations of the form:

$$iR[u] = i(\gamma u + \beta|u|^2u + \eta|u|^4u). \quad (2)$$

This perturbed NLS (PNLS) includes linear, cubic and quintic nonlinear gain/loss terms via the coefficients γ , β , and η , respectively. A positive coefficient corresponds to gain and a negative one to loss.

Our main tool for analyzing soliton interactions in the PNLS is based on the method first developed by Karpman and Solov'ev [23] for the 2-soliton interactions. Later this method was generalized to N -soliton interactions [24, 25, 26] with $iR[u] = 0$ and it was found that a chain of bright solitons can be accurately described (under the right assumptions) by a complex Toda chain (CTC). Further generalizations include treating the Manakov model (or vector NLS equation), as well as treating the effects of various perturbations (mainly external potentials), see [27, 28, 29, 30, 31, 32] and the references therein. By extending the above methodologies to encompass the effects of linear and nonlinear (polynomial) gain/loss perturbation, we will derive effective equations of motion for a chain of bright solitons. These perturbations result in additional perturbative terms that modify the original CTC model. In Section 2 we derive the perturbed CTC (PCTC) taking into account the perturbations (2). In Section 3 we compare the predictions of the PCTC with the numerical solutions of the full PNLS. Finally, in Section 3.2 we present our conclusions and give possible avenues for further research.

2 DERIVATION OF THE PERTURBED COMPLEX TODA CHAIN

2.1 Derivation of the Generic Perturbed CTC

Lets us consider an N -soliton train as an initial condition to the perturbed NLS. By N -soliton train we mean a chain of several well-separated solitons whose parameters comply with the adiabatic approximation:

$$\begin{aligned} u(x, t = 0) &= \sum_{k=1}^N \vec{u}_k(x, t = 0), & u_k(x, t) &= \frac{2\nu_k e^{i\phi_k}}{\cosh(z_k)}, \\ z_k &= 2\nu_k(x - \xi_k(t)), & \xi_k(t) &= 2\mu_k t + \xi_{k,0}, \\ \phi_k &= \frac{\mu_k}{\nu_k} z_k + \delta_k(t), & \delta_k(t) &= 2(\mu_k^2 + \nu_k^2)t + \delta_{k,0}. \end{aligned} \quad (3)$$

For completeness, let us start by formulating the results of Karpman and Solov'ev's method [23] for general perturbation $R[u]$ and later specify the specific form for the perturbation (2). The adiabatic approximation holds true if the soliton parameters satisfy [23]:

$$|\nu_k - \nu_0| \ll \nu_0, \quad |\mu_k - \mu_0| \ll \mu_0, \quad |\nu_k - \nu_0| |\xi_{k+1,0} - \xi_{k,0}| \gg 1, \quad (4)$$

where $\nu_0 = \frac{1}{N} \sum_{k=1}^N \nu_k$ and $\mu_0 = \frac{1}{N} \sum_{k=1}^N \mu_k$ are, respectively, the average amplitude and velocity of the soliton chain. Thus, in the adiabatic approximation, one considers a chain of well-separated solitons with amplitudes and velocities that vary slightly from their averages. In fact, we define the following two scales:

$$|\nu_k - \nu_0| \approx \varepsilon_0^{1/2}, \quad |\mu_k - \mu_0| \approx \varepsilon_0^{1/2}, \quad |\xi_{k+1,0} - \xi_{k,0}| \approx \varepsilon_0^{-1}.$$

Skipping the details, we cast the perturbed CTC corresponding to generic perturbations $iR[u]$ [23]:

$$\begin{aligned} \frac{d\nu_k}{dt} &= 16\nu_0^3 \left(e^{-2\nu_0(\xi_{k+1} - \xi_k)} \sin(\delta'_{k+1} - \delta'_k) - e^{-2\nu_0(\xi_k - \xi_{k-1})} \sin(\delta'_k - \delta'_{k-1}) \right) + N_k[u], \\ \frac{d\mu_k}{dt} &= -16\nu_0^3 \left(e^{-2\nu_0(\xi_{k+1} - \xi_k)} \cos(\delta'_{k+1} - \delta'_k) - e^{-2\nu_0(\xi_k - \xi_{k-1})} \cos(\delta'_k - \delta'_{k-1}) \right) + M_k[u], \\ \frac{d\xi_k}{dt} &= 2\mu_k + \Xi_k[u], \quad \frac{d\delta_k}{dt} = 2(\nu_k^2 + \mu_k^2) + X_k[u], \end{aligned} \quad (5)$$

with $\delta'_k - \delta'_n = -2\mu_0(\xi_k - \xi_n) + \delta_k - \delta_n$, and where the perturbative terms are given by [23]:

$$\begin{aligned} N_k[u] &= \frac{1}{2} \text{Re} \int_{-\infty}^{\infty} \frac{dz_k}{\cosh z_k} R[u_k] e^{-i\phi_k}, & M_k[u] &= \frac{1}{2} \text{Im} \int_{-\infty}^{\infty} \frac{dz_k \tanh z_k}{\cosh z_k} R[u_k] e^{-i\phi_k}, \\ \Xi_k[u] &= \frac{1}{4\nu_k^2} \text{Re} \int_{-\infty}^{\infty} \frac{dz_k z_k}{\cosh z_k} R[u_k] e^{-i\phi_k}, & D_k[u] &= \frac{1}{2\nu_k} \text{Im} \int_{-\infty}^{\infty} \frac{dz_k (1 - z_k \tanh z_k)}{\cosh z_k} R[u_k] e^{-i\phi_k}, \end{aligned} \quad (6)$$

and $X_k[u] = 2\mu_k \Xi_k[u] + D_k[u]$. It is important to mention that, in deriving the PCTC, the following assumptions were used:

$$\xi_1 < \xi_2 < \dots < \xi_N; \quad \Delta_{k,k+1} = 2\nu_0(\xi_{k+1} - \xi_k), \quad e^{-|\Delta_{N,N+1}|} \equiv e^{-|\Delta_{0,1}|} \equiv 0;$$

as well as the following approximations:

$$\begin{aligned} z_k - z_n &\simeq 2\nu_0(x - \xi_k(t) - x + \xi_n(t)) \simeq -2\nu_0(\xi_{k0} - \xi_{n0}) = \Delta_{kn}, \\ \phi_k - \phi_n &\simeq \frac{\mu_0}{\nu_0}(z_k - z_n) + \delta_{k0} - \delta_{n0} \simeq -2\mu_0(\xi_{k0} - \xi_{n0}) + \delta_{k0} - \delta_{n0} = \delta'_k - \delta'_n, \end{aligned} \quad (7)$$

and, therefore, $e^{z_{k+1}} = e^{z_k} e^{-|\Delta_{k,k+1}|}$ and $e^{z_{k-1}} = e^{z_k} e^{|\Delta_{k,k-1}|}$. Also, we only keep terms of order of $\varepsilon_0 \simeq e^{-|\Delta_{kn}|}$ and neglect all terms of higher orders. Typically, the terms $\Xi_k[u]$ and $D_k[u]$ contribute to the right hand sides of Eqs. (5) with terms of the order of ε_0 that can be neglected as compared to the ‘leading’ terms $2\mu_k$ and $2(\mu_k^2 + \nu_k^2)$. Therefore, we finally obtain the generic perturbed CTC of the form:

$$\begin{aligned} \frac{d\lambda_k}{dt} &= -4\nu_0(e^{q_{k+1}-q_k} - e^{q_k-q_{k-1}}) + M_k + iN_k, & e^{q_1-q_0} &= 0, \quad e^{q_{N+1}-q_N} = 0, \\ \frac{dq_k}{dt} &= -4\nu_0\lambda_k + 2i(\mu_0 + i\nu_0)\Xi_k - iX_k, & k &= 1, \dots, N, \end{aligned} \quad (8)$$

where $\lambda_k = \mu_k + i\nu_k$, $X_k = 2\mu_k \Xi_k + D_k$ and

$$\begin{aligned} q_k &= -2\nu_0\xi_k + k \ln 4\nu_0^2 - i(\delta_k + \delta_0 + k\pi - 2\mu_0\xi_k), \\ \nu_0 &= \frac{1}{N} \sum_{s=1}^N \nu_s, \quad \mu_0 = \frac{1}{N} \sum_{s=1}^N \mu_s, \quad \delta_0 = \frac{1}{N} \sum_{s=1}^N \delta_s. \end{aligned} \quad (9)$$

Obviously, if no perturbation is present, $iR[u] = 0$, then $N_k = 0$, $M_k = 0$, $\Xi_k = 0$, $D_k = 0$ and the system (8) falls back to the original CTC.

2.2 The Effect of Linear and Nonlinear Gain/Loss on the CTC

Let us now calculate explicitly the terms N_k , M_k , Ξ_k and X_k corresponding to the specific perturbative terms as in Eq. (2). That means: (i) first in $iR[u]$ we have to replace u by $\sum_{p=1}^N u_p(x, t)$ and then, (ii) we have to sort the terms in the integrals for $N_k[u]$, \dots , $X_k[u]$ and, in particular, neglect the terms that are of order higher than ε_0 . Through this process, two different types of leading terms arise. The first type corresponds to ‘local’ (same k) terms involving:

$$R_k^{(0)}[u]e^{-i\phi_k} = \frac{2\nu_k}{\cosh(z_k)}\gamma + \frac{8\nu_k^3}{\cosh^3(z_k)}\beta + \frac{32\nu_k^5}{\cosh^5(z_k)}\eta. \quad (10)$$

The corresponding integrals can be straightforwardly computed with the result that only the integral $N_k[u]^{(0)}$ leads to a nonvanishing contribution:

$$N_k[u]^{(0)} = \frac{1}{2} \text{Re} \int_{-\infty}^{\infty} \frac{dz_k}{\cosh z_k} R[u_k]^{(0)} e^{-i\phi_k} = 2\nu_k \left(\gamma + \frac{8}{3}\beta\nu_k^2 + \frac{128}{15}\eta\nu_k^4 \right). \quad (11)$$

The other integrals in this approximation vanish:

$$\begin{aligned} M_k[u]^{(0)} &= \frac{1}{2} \text{Im} \int_{-\infty}^{\infty} \frac{dz_k \tanh z_k}{\cosh z_k} R[u_k]^{(0)} e^{-i\phi_k} = 0, & \Xi_k[u]^{(0)} &= \frac{1}{4\nu_k^2} \text{Re} \int_{-\infty}^{\infty} \frac{dz_k z_k}{\cosh z_k} R[u_k]^{(0)} e^{-i\phi_k} = 0, \\ D_k[u]^{(0)} &= \frac{1}{2\nu_k} \text{Im} \int_{-\infty}^{\infty} \frac{dz_k (1 - z_k \tanh z_k)}{\cosh z_k} R[u_k]^{(0)} e^{-i\phi_k} = 0. \end{aligned} \quad (12)$$

The second type of terms correspond to ‘nonlocal’ interaction terms between adjacent solitons. The perturbation linear in u obviously does not contribute to the ‘nonlocal’ terms $R_{k,n}^{(1)}[u]$. Since we only keep terms of order of ε_0 , we restrict our attention to nearest neighbor, $n = k \pm 1$, interactions. This yields the following interaction terms:

$$R_k^{(1)}[u] = \sum_{n=k\pm 1} \left[\beta (u_k^2 u_n^* + 2|u_k|^2 u_n) + \eta (2|u_k|^2 u_k^2 u_n^* + 3|u_k|^4 u_n) \right], \quad (13)$$

and, therefore,

$$R_k^{(1)}[u]e^{-i\phi_k} = \sum_{n=k\pm 1} \left[\beta \frac{8v_k^2 v_{k+1}}{\cosh^2(z_k) \cosh(z_{k+1})} \left(e^{i(\phi_k - \phi_{k+1})} + 2e^{-i(\phi_k - \phi_{k+1})} \right) + \eta \frac{32v_k^4 v_{k+1}}{\cosh^4(z_k) \cosh(z_{k+1})} \left(2e^{i(\phi_k - \phi_{k+1})} + 3e^{-i(\phi_k - \phi_{k+1})} \right) \right]. \quad (14)$$

Now, the integrations over space need to be performed. Keeping only the terms of order ε_0 yields (see the Appendix for details on the integrals involved):

$$N_k^{(1)}[u] \simeq 16v_0^3 \left(3\beta + \frac{40v_0^2}{3}\eta \right) \left(\cos(\delta'_k - \delta'_{k-1})e^{-|\Delta_{k,k-1}|} + \cos(\delta'_k - \delta'_{k+1})e^{-|\Delta_{k,k+1}|} \right), \quad (15)$$

$$M_k^{(1)}[u] \simeq \frac{16v_0^3}{3} \left(\beta + \frac{8v_0^2}{5}\eta \right) \left(\sin(\delta'_k - \delta'_{k-1})e^{-|\Delta_{k,k-1}|} - \sin(\delta'_k - \delta'_{k+1})e^{-|\Delta_{k,k+1}|} \right), \quad (16)$$

for $k = 2, \dots, N-1$ (i.e., solitons inside the chain) and, for solitons on the edges of the chain,

$$\begin{aligned} N_1^{(1)}[u] &= 16v_0^3 \left(3\beta + \frac{40v_0^2}{3}\eta \right) \cos(\delta'_1 - \delta'_2) e^{-|\Delta_{2,1}|}, & N_N^{(1)}[u] &= 16v_0^3 \left(3\beta + \frac{40v_0^2}{3}\eta \right) \cos(\delta'_N - \delta'_{N-1}) e^{-|\Delta_{N,N-1}|}, \\ M_1^{(1)}[u] &= -\frac{16v_0^3}{3} \left(\beta + \frac{8v_0^2}{5}\eta \right) \sin(\delta'_1 - \delta'_2) e^{-|\Delta_{2,1}|}, & M_N^{(1)}[u] &= \frac{16v_0^3}{3} \left(\beta + \frac{8v_0^2}{5}\eta \right) \sin(\delta'_N - \delta'_{N-1}) e^{-|\Delta_{N,N-1}|}. \end{aligned} \quad (17)$$

The $\Xi_k[u]^{(1)}$ and $D_k[u]^{(1)}$ contributions can also be calculated. However, as mentioned above, we will neglect them when compared to the leading terms $2\mu_k$ and $2(\mu_k^2 + v_k^2)$. Therefore, the relevant PCTC for N solitons takes the form:

$$\begin{aligned} \frac{d\lambda_1}{dt} &= -4v_0 e^{q_2 - q_1} + M_1 + iN_1, & \frac{d\lambda_N}{dt} &= 4v_0 e^{q_N - q_{N-1}} + M_N + iN_N, \\ \frac{d\lambda_k}{dt} &= -4v_0 (e^{q_{k+1} - q_k} - e^{q_k - q_{k-1}}) + M_k + iN_k, & k &= 2, \dots, N-1 \\ \frac{dq_k}{dt} &= -4v_0 \lambda_k, & \lambda_k &= \mu_k + iv_k. \end{aligned} \quad (18)$$

In order to render the mutual interactions between solitons more transparent, we explicitly cast the above PCTC for the special case of two solitons:

$$\begin{aligned} \frac{dv_1}{dt} &= 2v_1 P(v_1) + 16v_0^3 e^{-2v_0(\xi_2 - \xi_1)} \left(\sin(\delta'_1 - \delta'_2) + \left(3\beta + \frac{40v_0^2}{3}\eta \right) \cos(\delta'_1 - \delta'_2) \right), \\ \frac{dv_2}{dt} &= 2v_2 P(v_2) - 16v_0^3 e^{-2v_0(\xi_2 - \xi_1)} \left(\sin(\delta'_1 - \delta'_2) - \left(3\beta + \frac{40v_0^2}{3}\eta \right) \cos(\delta'_1 - \delta'_2) \right), \\ \frac{d\mu_1}{dt} &= 16v_0^3 e^{-2v_0(\xi_2 - \xi_1)} \left(\cos(\delta'_1 - \delta'_2) - \frac{1}{3} \left(\beta + \frac{8v_0^2}{5}\eta \right) \sin(\delta'_1 - \delta'_2) \right), \\ \frac{d\mu_2}{dt} &= -16v_0^3 e^{-2v_0(\xi_2 - \xi_1)} \left(\cos(\delta'_1 - \delta'_2) + \frac{1}{3} \left(\beta + \frac{8v_0^2}{5}\eta \right) \sin(\delta'_1 - \delta'_2) \right), \end{aligned} \quad (19)$$

and in addition:

$$\begin{aligned} \frac{d\xi_1}{dt} &= 2\mu_1, & \frac{d\delta_1}{dt} &= 2(\mu_1^2 + v_1^2), \\ \frac{d\xi_2}{dt} &= 2\mu_2, & \frac{d\delta_2}{dt} &= 2(\mu_2^2 + v_2^2), \end{aligned} \quad (20)$$

where the local dynamics for the soliton height is prescribed through

$$P(v_k) = \gamma + \frac{8}{3}\beta v_k^2 + \frac{128}{15}\eta v_k^4 = c_0 + c_1 v_k^2 + c_2 v_k^4. \quad (21)$$

It is important to mention that, unlike the CTC, the PCTC is not integrable. In particular, $v_1 + v_2 = 2v_0$ and $\mu_1 + \mu_2 = 2\mu_0$ now may depend on time.

2.3 Analysis of the Leading Terms in the PCTC

Let us first consider the leading terms responsible for the perturbations in the chain. Specifically, these leading terms affect all the amplitudes of the solitons:

$$\frac{dv_k}{dt} = 2v_k P(v_k), \quad (22)$$

where $P(v)$ is defined above in Eq. (21). Focusing on the above leading terms (only present in the soliton amplitudes), there are two classes of solutions corresponding to the following two choices of the perturbation parameters γ , β and η :

$$\begin{aligned} \text{(a)} \quad & c_1^2 - 4c_2c_0 > 0, \quad \text{i.e., } P(v_k) \text{ has 4 real roots,} \\ \text{(b)} \quad & c_1^2 - 4c_2c_0 < 0, \quad \text{i.e., } P(v_k) \text{ has 2 pairs of mutually complex conjugate roots.} \end{aligned} \quad (23)$$

For practical applications one needs to restrict parameters such that the solution for v_k which remains ‘physical’ (i.e., does not blow up or vanish quickly) for long times. The relevant condition (a) or (b) will provide a constraint for the perturbation parameters which ensure such behavior of v_k . Such analysis would be interesting and will be left to a future publication. Nonetheless, in what follows, we consider in more detail the case $\eta = 0$ where the quintic gain/loss term is absent. Thus, in the absence of quintic gain/loss, the leading terms of the perturbations, corresponding to purely cubic gain/loss and a combination of linear and cubic gain/loss case, yield, respectively:

$$\text{(A)} \quad \frac{dv_k}{dt} = \frac{16\beta}{3}v_k^3, \quad (24)$$

$$\text{(B)} \quad \frac{dv_k}{dt} = 2\gamma v_k + \frac{16\beta}{3}v_k^3. \quad (25)$$

It is evident that the gain/loss coefficients affect strongly the amplitudes of the solitons. In fact, the above systems have the following explicit solutions:

$$\text{(A)} \quad v_k(t) = \frac{3}{\sqrt{9C_0 - 96\beta t}}, \quad (26)$$

$$\text{(B)} \quad v_k(t) = \sqrt{\frac{3\gamma}{3\gamma C_1 \exp(-4\gamma t) - 8\beta}}, \quad (27)$$

where the integration constants C_0 and C_1 are determined by the initial soliton heights.

This means, as mentioned above, that the average amplitude v_0 is no longer constant, but depends on t . Therefore, for generic choices of β and γ , the amplitudes v_k may decrease or increase substantially, which is not compatible with the adiabatic approximation.

3 NUMERICAL RESULTS

3.1 Soliton Amplitude Dynamics

Before focusing on the soliton chain, let us consider the leading term in the PCTC system: the decay/growth of the soliton amplitude. Therefore, let us consider first a single soliton and follow its evolution according to the PCTC. Figure 1 depicts the comparison of the analytical solutions (26) and (27) and full numerical simulations of the perturbed NLS (1)-(2). The full numerical PDE solutions were obtained by integrating an initial bright soliton solution of the form (3) (i.e., the solution when no gain/loss terms are present) using a combination of second order finite-differences in space and Runge-Kutta in time. We typically used the spatial domain $[-80, 80]$ with 1024 spatial mesh points and a temporal time step of $\Delta t = 0.0025$ to ensure numerical stability [33]. The PCTC numerics were obtained using the ode45 package in Matlab. Figure 1(a) depicts the evolution of the soliton height for the case when only the cubic loss/gain term is present ($\gamma = \eta = 0$) for different values of the cubic coefficient including gain ($\beta > 0$) and loss ($\beta < 0$) and for an initial soliton of initial height $2v(0) = 1$. As the panels shows, there is very good agreement between the perturbative solution (line) and the full PDE dynamics (circles) for both cubic gain ($\beta > 0$) and loss ($\beta < 0$). Similarly, Figure 1(b) depicts a similar scenario when both linear gain and cubic loss are present. In this case we fix $\gamma = 0.001$ and $\beta = -0.01$ and vary the initial height of the seeded soliton. As expected, the soliton evolves towards the steady

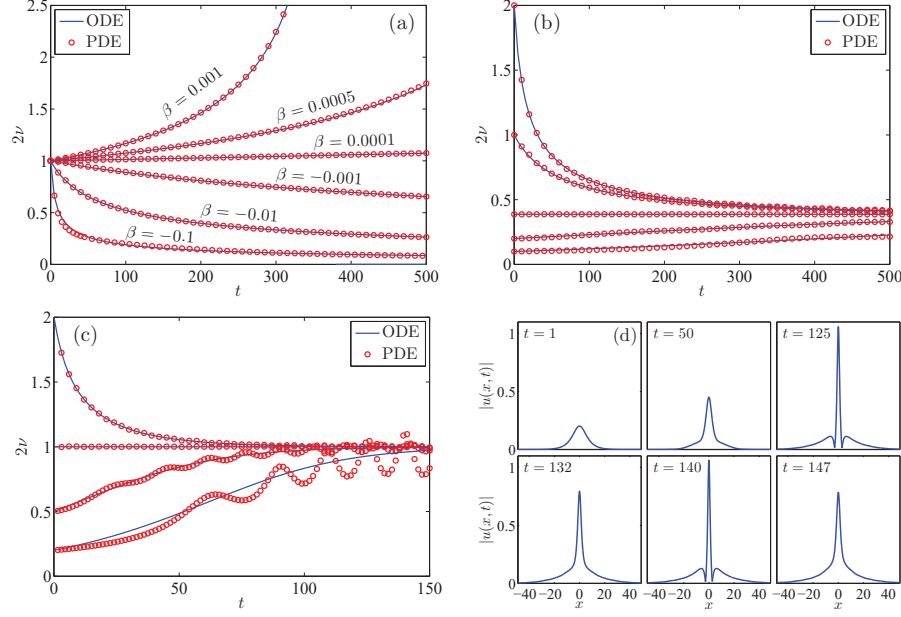


FIGURE 1. Growth/decay for a single soliton in the presence of higher order loss/gain terms. The solid (blue) lines correspond to the analytical solutions (26) and (27) for, respectively, the ODE models (24) and (25), while the (red) circles correspond to full numerical PDE solutions of the perturbed NLS (1)-(2). The numerical PDE solutions were started with the exact soliton solution in the absence of any gain/loss terms (*i.e.*, solution (3)). **(a)** Only the cubic loss/gain is present ($\gamma = \eta = 0$). The different values for the cubic gain/loss are indicated where $\beta > 0$ and $\beta < 0$ correspond, respectively, to gain and loss. All the initial solitons were seeded with height $2\nu = 1$. **(b)** Soliton amplitude for linear gain and cubic loss corresponding to $\gamma = 0.001$ and $\beta = -0.01$. Each curve corresponds to initializing the system with a soliton of a different amplitude: $\nu(t=0) = \frac{1}{2}(2, 1, 0.3863, 0.2, 0.1)$ from top to bottom. The value $2\nu = \sqrt{3/5}/2 \approx 0.3863$ corresponds to the fixed point ν_∞ of Eq. (25). **(c)** Same as in panel (b) but for $\gamma = 0.01$ and $\beta = -1.5\gamma$ and initial amplitude $\nu(t=0) = \frac{1}{2}(2, 1, 0.5, 0.2)$. **(d)** Dynamics of the full PDE evolution starting with the soliton solution with $\nu(0) = \frac{1}{2}0.2 < \nu_\infty = 1$. The snapshots show the magnitude of the field $|u(x, t)|$ at the indicated times. The integration domain is $[-80, 80]$ while the plotting range is the subset $[-49, 49]$

state height given by the, non-trivial, fixed point solution $\nu_\infty \equiv \nu(t \rightarrow \infty) = \sqrt{\frac{3\gamma}{-8\beta}}$. In Figure 1(c) we depict a very similar scenario as the one for Figure 1(b) but for the larger value of the nonlinear gain/loss parameters: $\gamma = 0.01$ and $\beta = -1.5\gamma$. In this case, when the amplitude of the soliton is higher, or slightly lower, than $\nu_\infty = 1/2$ there is again excellent agreement between the ODE model and the PDE dynamics. However, when the initial height of the soliton is small, the soliton grows and starts developing oscillations in the tails (and the height) as shown in panel (d). This is due to the fact that we are initializing our PDE system with a soliton solution of the NLS without gain/loss terms. As a result the wings of the soliton unexpectedly acquire mass and induce the oscillations. These oscillations are long-lived but transitory as the system eventually settles to the exact soliton solution corresponding to the parameter values at hand. Nonetheless, despite the spurious oscillations, the PDE dynamics follows the main trend of the ODE model as expected.

It is important to mention at this stage that the PDE dynamics for the case of linear gain and cubic loss is always unstable as the zero background solution $u(x, t) = 0$, where the solitons are embedded, suffers from modulational instability due to the linear gain. In all of the relevant results with linear gain presented above and below, we are assuming that this instability is weak and therefore negligible. In fact, in all numerical experiments reported here, no instability of the background state was visible on the time scale of our runs. A natural way to rid the system of the inherent modulational instability of the background state is to treat the full linear, cubic, and quintic gain/loss model with (i) a linear loss that suppresses the modulational instability of the background state and (ii) a competition of a

cubic gain and a quintic loss so that stable solitons can ensue [35]. This topic falls outside the scope of the current manuscript and it is currently under investigation; the relevant results will be published elsewhere.

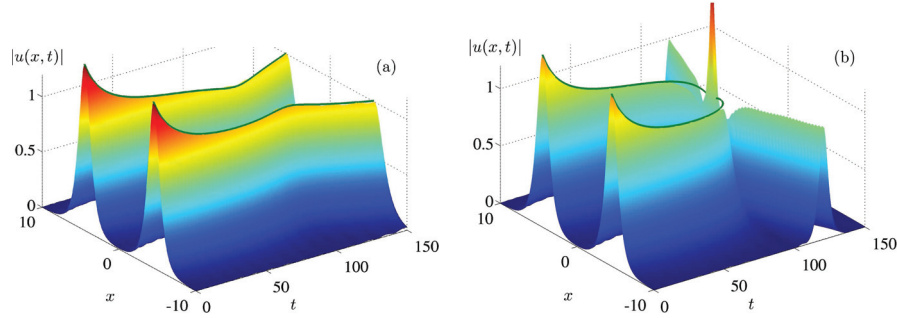


FIGURE 2. Soliton-soliton interaction dynamics. Shown are the surface plots of $|u(x, t)|$ vs. (x, t) obtained from the full integration of the NLS (1). We also depict, see (green) thick curve closely following the peak of the solitons, for the same initial conditions, the corresponding reduced dynamics of the PCTC (19)-(20). The parameters of the NLS are given by: $\gamma = 0.01$, $\beta = -1.5\gamma$, and $\eta = 0$. Panel (a) corresponds to two solitons with initial conditions: $\xi_1(0) = -4.5$, $\xi_2(0) = +4.5$, $2\nu_1(0) = 2\nu_2(0) = 1.5$ (corresponding to solitons that are 50% higher than the steady state height $2\nu_\infty = 1$), $\mu_1(0) = \mu_2(0) = 0$, and $\delta_2(0) - \delta_1(0) = 0.2$. Panel (b) has the same initial condition as in panel (a) with the exception that $\delta_2(0) - \delta_1(0) = 0$; namely, the two solitons are initially in phase. Note the excellent agreement between the full NLS numerics and the reduced PCTC model

3.2 Soliton-Soliton Interactions

Having shown in the previous section that the local amplitude dynamics under the presence of linear and cubic gain/loss terms prescribed by perturbation is an accurate model for a single soliton, we now turn our attention to the dynamics of soliton interactions. In the interest of brevity, we will compare the reduced perturbation dynamics with the full NLS evolution for a pairwise interaction between two solitons. Therefore, let us focus on the system of equations (19)-(20) describing the soliton parameters evolution for two well-spaced solitons. Figure 2 depicts two typical scenarios for the interaction dynamics between two solitons. Panel (a) depicts the case of two solitons with heights higher than the equilibrium $2\nu_\infty$ and with a relative phase shift of 0.2π . As the panel shows, the dynamics of the full NLS numerical solution (see colored surface plot) is in excellent agreement with the reduced dynamics (19)-(20) shown by the (green) thick curve following the peak of the solitons. Similarly, in panel (b) we show the case corresponding to the same initial condition as in panel (a) but with the initial relative phase being zero. In this case as well, the reduced dynamics is in excellent agreement with the full NLS numerics for times before the collision between solitons. As our reduced ODEs are not valid (during or) after the collision, we stop the ODE dynamics when the solitons collide.

In order to compare in a more qualitative manner the full NLS dynamics and the reduced PCTC model, we have also extracted the shape parameters of the NLS solitons by performing a standard nonlinear square fitting routine to each snapshot with an ansatz consisting of the sum of two bright solitons of the form (3). Figure 3 presents a couple of typical cases where the NLS parameters extracted by the above fitting are depicted by small circles and the reduced PCTC results are depicted by the colored solid curves. For guidance, we also include (see thin black curves) the corresponding results when the gain/loss terms are absent ($\gamma = \beta = \eta = 0$). Figure 3(a) corresponds to the case shown in panel (a) of Figure 2. As it is clear from this panel, despite some oscillations in the full NLS dynamics, the soliton height from the reduced PCTC model is in very good agreement with the full NLS numerics. These small oscillations of the amplitude (and width) of the NLS solitons are similar to the ones described previously for Fig. 1(c)-(d) and are, naturally, absent in the PCTC model. Nonetheless, despite the oscillations, the main trend (after averaging out the oscillations) is very well described by the reduced PCTC. Also note the contrast between the Hamiltonian dynamics when all loss/gain terms are absent (see thin black lines). Panel (b) in Figure 3 depicts a similar scenario to panel (a) but where the solitons are initialized with the precise equilibrium height $2\nu_\infty$. Again, as in the previous case, there is very good agreement between the full NLS model and its corresponding PCTC ODE reduction. It is interesting that although in this case we start with the correct height for the solitons, the shape is still not very close to the exact

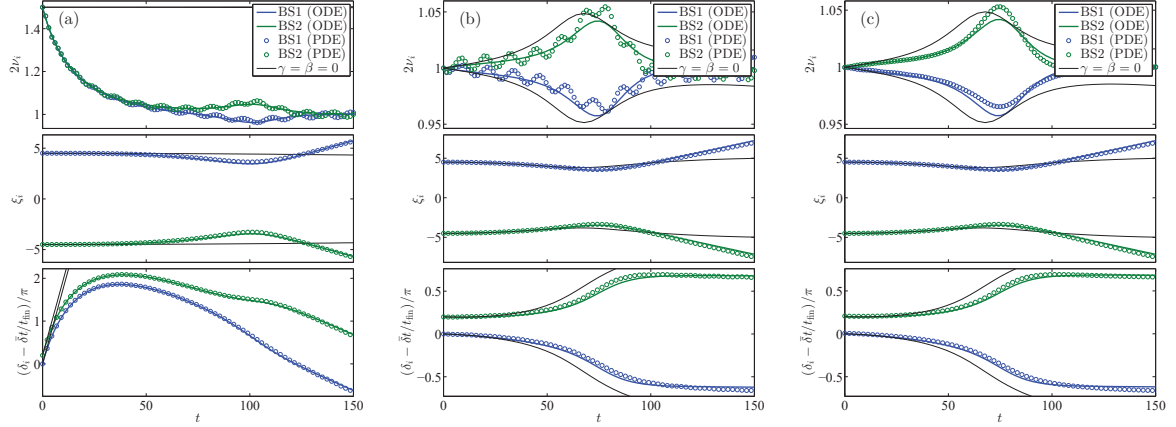


FIGURE 3. Comparing the soliton-soliton dynamics between the full NLS model and its PCTC reduction. The different panels depict soliton shape parameters: height (top), position (middle), and phase (bottom) for two interacting solitons. The thick colored lines correspond to the PCTC ODE model while the the circle to the full NLS PDE numerics. The shape parameter for the NLS numerics are extracted by numerically fitting the ansatz (3). For all the cases we chose $\gamma = 0.01$, $\beta = -1.5\gamma$, and $\eta = 0$. Also, for comparison, the thin black curves correspond to the Hamiltonian case $\gamma = \beta = \eta = 0$. The different cases correspond to the set following of initial conditions. **(a)** $\xi_1(0) = -4.5$, $\xi_2(0) = +4.5$, $2v_1(0) = 2v_2(0) = 1.5$ (corresponding to solitons that are 50% higher than the steady state height $2v_\infty = 1$), $\mu_1(0) = \mu_2(0) = 0$, and $\delta_2(0) - \delta_1(0) = 0.2$. **(b)** Same as in panel (a) but with $2v_1(0) = 2v_2(0) = 2v_\infty = 1$, corresponding to solitons with a height equal to the steady state height. In panels (a) and (b) the initial condition for the NLS PDE is constructed using the ansatz (3). **(c)** Same as in panel (b) but in this case we initialize each NLS PDE soliton with the numerically exact one-soliton solution obtained using the nonlinear Newton-Krylov solver `nsoli` [34]. Then, the two solitons are seeded by displacing this numerically exact profile to the initial positions and imprinting their phases as necessary by multiplying (before adding them together) each soliton by its corresponding $e^{i\delta_k(0)}$ phase term

solution as our ansatz (3) is not an exact solution for the steady state with linear gain and cubic loss. In fact, by applying a standard fixed point algorithm, we have found the numerically exact steady states for given choices of the gain/loss parameters. After using this numerically exact profile and seeding it in the NLS numerical integrator at the desired location with the desired phases (by multiplying each soliton by its corresponding $e^{i\delta_k(0)}$ phase term), we are able to initialize the system with solitons that do not display the oscillation in height (and width) present in the previous two cases. The dynamics corresponding to the same case as in Figure 3(b), but by using the numerically exact solitons when the gain/loss parameters are present, is depicted in Figure 3(c). This panel shows that the height oscillations are now nicely suppressed.

CONCLUSIONS AND OUTLOOK

We have derived reduced equations of motion for chains of bright solitons in the NLS perturbed with linear and non-linear gain/loss terms. By generalizing the soliton perturbation methodology, we have obtained a perturbed complex Toda chain (PCTC) for the soliton's shape parameters (height, width, positions, velocity, and phase). The dynamics of this PCTC is in very good agreement with the full numerics of the original perturbed NLS model. In particular, we have corroborated that the PCTC is indeed in very good agreement for the case of (i) single soliton solutions and (ii) soliton-soliton interactions. For these single soliton solutions, we have observed that starting away from the steady state height $2v_\infty$ (where linear gain is balanced by cubic loss) induces a relaxation dynamics towards the equilibrium $2v_\infty$. We have also observed that, starting with solitons in the full NLS model with heights below $2v_\infty$, induces oscillations in the soliton's height (and width). It would be interesting to find whether these oscillation could be eliminated by starting with a modified soliton profile. Indeed, we were able to eliminate these oscillations by starting with the numerically exact steady state profile. However, the generalization of this to transient dynamics (particularly when a small soliton grows towards the steady state height) may require further work.

It would be interesting to study in more detail the limitations of the PCTC, particularly when more than two

solitons are interacting. For instance, the toy model that we used hereby has the limitation that the zero background level is always unstable due to the modulational instability induced by the linear gain (which dominates for small field amplitudes). However, it is worth mentioning that our perturbation approach can also be carried out with quintic gain/loss terms. It would be interesting to analyze this more general class of models and its PCTC reductions. Particularly important is the case corresponding to linear loss, cubic gain, and quintic loss [35] as this produces a stable zero background (due to linear loss) and a fixed point soliton height where the cubic gain and quintic loss are balanced. This topic is currently under investigation and will be reported in a future publication.

Another avenue of possible research would be to apply the non-conservative variational approximation for NLS [36] to obtain correction terms in the soliton-soliton interaction that originate from the deviation of a sech-soliton shape when gain and loss are present [37]. It will be important to check also whether the PCTC model describes adequately the interactions of three or more solitons. Finally, another interesting trend would be to derive the PCTC model (18) for the Manakov system with gain/loss perturbations, see Refs. [27, 28, 29, 30, 31, 32, 38]. Our hypothesis is that the adiabatic approximation would apply to the N -soliton interactions provided the gain and loss terms balance each other so that the soliton amplitudes stay bounded in a small interval around their average value.

ACKNOWLEDGEMENTS

MDT acknowledges Bulgarian Scientific Fund under grant DFNI I-02/9.

A TYPICAL INTEGRALS

Here we list the typical integrals that appear in deriving the PCTC. First we list the integrals

$$\int_{-\infty}^{\infty} \frac{dz}{\cosh^2(z)} = 2, \quad \int_{-\infty}^{\infty} \frac{dz}{\cosh^4(z)} = \frac{4}{3}, \quad \int_{-\infty}^{\infty} \frac{dz}{\cosh^6(z)} = \frac{16}{15}. \quad (28)$$

needed to derive $R_k[u]^{(0)}$. It is possible to derive analytical expressions for all integrals $R_k[u]^{(1)}$, but these turn out to be very involved. Below we are keeping only terms of the order of ε_0 :

$$\begin{aligned} \int_{-\infty}^{\infty} \frac{dz_k}{\cosh^3(z_k) \cosh(z_{k\pm 1})} &= 4e^{-|\Delta_{k,k\pm 1}|} + \mathcal{O}(\varepsilon_0^{3/2}), & \int_{-\infty}^{\infty} \frac{dz_k}{\cosh^5(z_k) \cosh(z_{k\pm 1})} &= \frac{8}{3}e^{-|\Delta_{k,k\pm 1}|} + \mathcal{O}(\varepsilon_0^{3/2}), \\ \int_{-\infty}^{\infty} \frac{dz_k \tanh(z_k)}{\cosh^3(z_k) \cosh(z_{k\pm 1})} &= \mp \frac{4}{3}e^{-|\Delta_{k,k\pm 1}|} + \mathcal{O}(\varepsilon_0^{3/2}), & \int_{-\infty}^{\infty} \frac{dz_k \tanh(z_k)}{\cosh^5(z_k) \cosh(z_{k\pm 1})} &= \mp \frac{8}{15}e^{-|\Delta_{k,k\pm 1}|} + \mathcal{O}(\varepsilon_0^{3/2}), \\ \int_{-\infty}^{\infty} \frac{dz_k z_k}{\cosh^3(z_k) \cosh(z_{k\pm 1})} &= \mp 2e^{-|\Delta_{k,k\pm 1}|} + \mathcal{O}(\varepsilon_0^{3/2}), & \int_{-\infty}^{\infty} \frac{dz_k z_k}{\cosh^5(z_k) \cosh(z_{k\pm 1})} &= \mp \frac{2}{3}e^{-|\Delta_{k,k\pm 1}|} + \mathcal{O}(\varepsilon_0^{3/2}), \\ \int_{-\infty}^{\infty} \frac{dz_k (1 - z_k \tanh(z_k))}{\cosh^3(z_k) \cosh(z_{k\pm 1})} &= 2e^{-|\Delta_{k,k\pm 1}|} + \mathcal{O}(\varepsilon_0^{3/2}), & \int_{-\infty}^{\infty} \frac{dz_k (1 - z_k \tanh(z_k))}{\cosh^5(z_k) \cosh(z_{k\pm 1})} &= 2e^{-|\Delta_{k,k\pm 1}|} + \mathcal{O}(\varepsilon_0^{3/2}). \end{aligned} \quad (29)$$

REFERENCES

- [1] C. Sulem and P. L. Sulem, *The Nonlinear Schrödinger Equation* (Springer-Verlag, New York, 1999).
- [2] R. K. Dodd, J. C. Eilbeck, J. D. Gibbon, and H. C. Morris, *Solitons and Nonlinear Wave Equations* (Academic, New York, 1983).
- [3] M. J. Ablowitz, B. Prinari, and A. D. Trubatch, *Discrete and Continuous Nonlinear Schrödinger Systems* (Cambridge University Press, Cambridge, 2004).
- [4] J. Bourgain, *Global Solutions of Nonlinear Schrödinger Equations* (American Mathematical Society, Providence, 1999).
- [5] M. J. Ablowitz, *Nonlinear Dispersive Waves. Asymptotic Analysis and Solitons* (Cambridge University Press, 2011).
- [6] A. Hasegawa, *Optical Solitons in Fibers* (Springer-Verlag, Heidelberg, 1990).
- [7] F. Kh. Abdullaev, S. A. Darmanyan, and P. K. Khabibullaev, *Optical Solitons* (Springer-Verlag, Heidelberg, 1993).

- [8] A. Hasegawa and Y. Kodama, *Solitons in Optical Communications* (Clarendon Press, Oxford, 1995).
- [9] Yu. S. Kivshar and G. P. Agrawal, *Optical Solitons: From Fibers to Photonic Crystals* (Academic Press, 2003).
- [10] C. J. Pethick and H. Smith, *Bose-Einstein Condensation in Dilute Gases* (Cambridge University Press, Cambridge, 2002).
- [11] L. P. Pitaevskii and S. Stringari, *Bose-Einstein Condensation*, (Oxford University Press, Oxford, 2003).
- [12] P. G. Kevrekidis, D. J. Frantzeskakis, and R. Carretero-González (Eds.), *Emergent Nonlinear Phenomena in Bose-Einstein Condensates. Theory and Experiment* (Springer-Verlag, Berlin, 2008); R. Carretero-González, D. J. Frantzeskakis, and P. G. Kevrekidis (2008) *Nonlinearity* **21**, R139.
- [13] P. G. Kevrekidis, D. J. Frantzeskakis and R. Carretero-González, *The Defocusing Nonlinear Schrödinger Equation*, (SIAM, Philadelphia, 2015).
- [14] E. Infeld and G. Rowlands, *Nonlinear Waves, Solitons and Chaos* (Cambridge University Press, Cambridge, 1990).
- [15] W. van Saarloos and P. C. Hohenberg (1992) *Physica D* **56**, 303.
- [16] I. S. Aranson and L. Kramer (2002) *Rev. Mod. Phys.* **74**, 99.
- [17] M. C. Cross and P. C. Hohenberg (1993) *Rev. Mod. Phys.* **65**, 851.
- [18] A. Scott, *Nonlinear Science. Emergence and Dynamics of Coherent Structures*, 2nd edn (Oxford University Press, Oxford, 2003).
- [19] M. J. Ablowitz and H. Segur, *Solitons and the Inverse Scattering Transform* (SIAM, Philadelphia, 1981).
- [20] V. E. Zakharov, S. V. Manakov, S. P. Nonikov, and L. P. Pitaevskii, *Theory of Solitons* (Consultants Bureau, NY, 1984).
- [21] A. C. Newell, *Solitons in Mathematics and Physics* (SIAM, Philadelphia, 1985).
- [22] V. S. Gerdjikov, “Basic aspects of soliton theory,” in *Geometry, Integrability and Quantization*, I. M. Mladenov, A. C. Hirshfeld (Eds.), (Softex, Sofia, 2005), pp. 78–125, nlin.SI/0604004.
- [23] V. I. Karpman and V. V. Solov’ev (1981) *Physica D* **3D**, 487; V. I. Karpman (1979) *Physica Scripta* **20**, 462–478.
- [24] V. S. Gerdjikov, D. J. Kaup, I. M. Uzunov, and E. G. Evstatiev (1996) *Phys. Rev. Lett.* **77**, 3943–3946.
- [25] V. S. Gerdjikov, I. M. Uzunov, E. G. Evstatiev, and G. L. Diankov (1997) *Phys. Rev.* **E55**, 6039–6060.
- [26] V. S. Gerdjikov, E. G. Evstatiev, D. J. Kaup, G. L. Diankov, and I. M. Uzunov (1998) *Phys. Lett.* **A241**, 323–328.
- [27] V. S. Gerdjikov, “ N -soliton interactions, the Complex Toda Chain and stability of NLS soliton trains,” in *Proceedings of the International Symposium on Electromagnetic Theory*, Vol. 1, E. Kriezis (Ed.), (Aristotle University of Thessaloniki, Greece, 1998), pp. 307–309; V. S. Gerdjikov, “Complex Toda Chain – an integrable universal model for adiabatic N -soliton interactions,” in *Nonlinear Physics: Theory and Experiment. II*, M. Ablowitz, M. Boiti, F. Pempinelli, B. Prinari (Eds.), (World Scientific, 2003), pp. 64–70.
- [28] V. S. Gerdjikov, E. V. Doktorov, and N. P. Matsuka (2007) *Theor. Math. Phys.* **151**, 762–773.
- [29] V. S. Gerdjikov, N. A. Kostov, E. V. Doktorov, and N. P. Matsuka (2009) *Math. Comput. Simulat.* **80**, 112–119.
- [30] V. S. Gerdjikov and M. D. Todorov, “ N -soliton interactions for the Manakov system: Effects of external potentials,” Chapter in *Localized Excitations in Nonlinear Complex Systems, Nonlinear Systems and Complexity 7*, P. Kevrekidis *et al* (Eds.), (Springer International Publishing, Switzerland, 2014), pp. 147–169.
- [31] V. S. Gerdjikov, M. D. Todorov, and A. V. Kyuldjiev, “Polarization effects in modeling soliton interactions of the Manakov model,” in *AMiTaNS’15*, AIP Conference Proceedings 1684, edited by M. D. Todorov, (American Institute of Physics, Melville, NY, 2015), paper 080006, 12p.
- [32] V. S. Gerdjikov, M. D. Todorov, and A. V. Kyuldjiev (2017) *Wave Motion* **71**, 71–81, Special Issue “Mathematical modeling and physical dynamics of solitary waves: From continuum mechanics to field theory,” I. C. Christov, M. D. Todorov, and S. Yoshida (Guest Eds.).
- [33] R. M. Caplan and R. Carretero-González (2013) *Appl. Num. Math.* **71**, 24–40.
- [34] C. T. Kelley, *Solving Nonlinear Equations with Newton’s Method. Fundamentals of Algorithms* (SIAM, 2003).
- [35] V. V. Afanasjev (1995) *Optics Letters* **20**, 704–706.
- [36] J. Rossi, R. Carretero-González, and P. G. Kevrekidis. *Non-conservative variational approximation for nonlinear Schrödinger equations*, in preparation.
- [37] J. Rossi, R. Carretero-González, P. G. Kevrekidis, and M. Haragus (2016) *J. Phys.* **A49**, 455201.
- [38] V. S. Gerdjikov, M. D. Todorov, and A. V. Kyuldjiev (2016) *Math. Comput. Simulat.* **121**, 166–178.